

## INTERLAYER STRUCTURE AND DYNAMICS OF ALKYLAMMONIUM-INTERCALATED SMECTITES WITH AND WITHOUT WATER: A MOLECULAR DYNAMICS STUDY

XIANDONG LIU, XIANCAI LU\*, RUCHENG WANG, HUIQUN ZHOU AND SHIJIN XU

State Key Laboratory of Mineral Deposit Research, Department of Earth Sciences, Nanjing University, Hankou Road 22, Nanjing 210093, PR China

**Abstract**—The structure and dynamics of alkylammonium-intercalated smectites were simulated using molecular dynamics employing the clayff-CVFF force field, the reliability of which was firstly validated for these systems. The layering behaviors of alkyl chains confirm the scenarios of the monolayer, transition and bilayer configurations for short, medium-length and long carbon tails, respectively. In the systems without water, the alkylammonium groups are all anchored firmly above the surface six-member rings through H bonds between ammonium hydrogen and surface oxygen, and the alkyl tails are a little more mobile. With water involved, some ammoniums are dragged out of the potential barriers of the six-member rings by water molecules through the strong H bonds between water oxygen and ammonium hydrogen. The intercalated water scarcely affects the basal spacing, alkyl chain layering or alkylammonium dynamics. It is also found that the systems with alkyl chains of 11 to 14 exhibit the greatest density, resulting in the extremely limited mobility of the intercalated species.

**Key Words**—Alkylammonium, Intercalation, Molecular Dynamic, Smectite, Swelling.

### INTRODUCTION

The intercalation of alkylammonium surfactants into phyllosilicates has attracted great interest in terms of both applied and basic research (Lagaly *et al.*, 2006). In the preparation of polymer-clay nanocomposites (PCNs), alkylammonium species are principally used as modifiers to make the interlayer spaces of silicates organophilic, and such modification promotes the entrance of polymers (Lagaly *et al.*, 2006). The organophilic properties of the alkylammonium-intercalated phyllosilicates can also be used to remove organic pollutants from water (Carrizosa *et al.*, 2004). Furthermore, intercalation of alkylammonium ions is often used to derive the layer-charge information of phyllosilicates (Lagaly, 1981, 1994; Laird, 1994; Laird *et al.*, 1989; Mermut and Lagaly, 2001), and also employed as an ideal model to explore the confinement effects induced by the nano-sized interlayer pores due to the relatively simple molecular structures of the alkylammonium species (Horn and Israelachvili, 1981; Hackett *et al.*, 1998).

Many experimental studies have focused on the alkylammonium-intercalated clays. Based on the basal spacing data from X-ray diffraction (XRD) measurements, it is deduced that the arrangements of intercalated ions are controlled by both the electrostatics of phyllosilicates and the length of the alkyl chain (Janek and Smrcok, 1999; Lagaly, 1981; Laird *et al.*, 1989;

Weiss, 1963). Several ideal arrangement structures have been proposed: short-chain alkylammonium ions usually tend to form monolayers, the longer ones arrange to bilayers; pseudo-trilayers are usually formed within highly-charged phyllosilicates, and paraffin structures are formed by the alkylammonium ions with two or more long alkyl chains (Lagaly *et al.*, 2006). Fourier transform infrared (FTIR) spectroscopy (Vaia *et al.*, 1994; Osman *et al.*, 2000, 2002, 2004; Zhu *et al.*, 2005) and nuclear magnetic resonance (NMR) spectroscopy (Osman *et al.*, 2002, 2004; Wang *et al.*, 2000; Zhu *et al.*, 2005) have revealed that disordered (mixture of *trans* and *gauche*) and ordered (all *trans*) conformations can coexist in organic phases.

Molecular simulation has been proven to be a powerful tool to complement experiments in the physical chemistry of complex systems (Allen and Tildesley, 1987; Frenkel and Smit, 2002). To date, however, there have only been a few simulation studies on smectite-alkylammonium systems. Zeng *et al.* (2003, 2004) studied these systems by using the force field of Skipper *et al.* (1995) and the UA (united-atom) Dreiding force field (Mayo *et al.*, 1990) to describe the clay and organic ions, respectively. Tambach *et al.* (2006) investigated the swelling behaviors and the conformations of intercalated alkylammoniums by combining the force field of Skipper with OPLS-UA (OPLS united-atom) (Jorgensen *et al.*, 1984, 1986). Some simulations focused on the systems intercalated by alkylammoniums with very long chains (He *et al.*, 2005; Heinz *et al.*, 2003, 2005, 2007). All of these simulations reproduced XRD measurements and verified the layering behavior of alkyl chains. However, some

\* E-mail address of corresponding author:

xcljun@nju.edu.cn

DOI: 10.1346/CCMN.2007.0550602

important issues remain unresolved. Recently, thermogravimetric analysis (TGA) has indicated that the organic-intercalated materials often contain water and water can interact strongly with the intercalated polymers, which may influence the material properties (Boulet *et al.*, 2003; Greenwell *et al.*, 2005). However, the effects of water have often been omitted in previous simulations of alkylammonium-intercalated phyllosilicates. Moreover, the bonding between alkylammonium and clay has not been well represented, especially with the use of the UA-type force fields. For example, in the simulations of Zeng *et al.* (2003, 2004), the ammonium group was modeled as a positively charged ‘united atom’, so it is impossible to understand the interactions between the ammonium H and surface O, which have been deduced from experiments (Lagaly and Weiss, 1970).

The advanced force fields can effectively facilitate classical molecular simulation studies. The clayff (Cygan *et al.*, 2004b), parameterized by incorporating both the quantum-mechanical calculations and structural data of model mineral phases, has been validated in simulations of oxides, oxyhydroxides, clay minerals and their interfaces with aqueous solutions (*e.g.* Cygan *et al.*, 2004a, 2004b; Greathouse *et al.*, 2005; Kirkpatrick *et al.*, 2005; Wang *et al.*, 2004, 2006; Liu and Lu, 2006). It has been suggested that the clayff can be integrated with the CVFF (consistent valence force field) (Dauber-Osguthorpe *et al.*, 1988) to simulate the hybrid systems of inorganic minerals and organic matter, and many systems have been simulated successfully (Kumar *et al.*, 2006; Cygan *et al.*, 2004a).

In this study, we employ the clayff-CVFF in systematic simulations of the alkylammonium-intercalated smectites and aim to investigate the interlayer structures and dynamics at the atomic level and to uncover the effects of water. At first, we derived the swelling curve of the smectites intercalated by alkylammoniums of alkyl chains of C<sub>6</sub> to C<sub>18</sub>. The good agreement between the simulated swelling curve and the available XRD data validates the reliability of the combined force field. Then we studied the structural and dynamic properties of the systems with respective intercalations of C<sub>6</sub>, C<sub>12</sub> and C<sub>18</sub> ions, with and without the presence of water. The layering behavior of alkyl chains, interlayer bonding and the dynamics are uncovered at the atomic level and the effects of water are addressed in detail.

## METHODS

### Organoclay model

Wyoming-type montmorillonite (Skipper *et al.*, 1995; Tambach *et al.*, 2004), the chemical formula of which is  $X_{0.625}[Si_{7.875}Al_{0.125}][Al_{3.5}Mg_{0.5}]O_{20}(OH)_4$  where  $X$  represents interlayer compensation cations, was used for the simulation. This model has 0.625  $e$  per unit-cell, consisting of 0.125 tetrahedral charges and 0.5 octa-

hedral charges. The isomorphic substitutions in clay sheets obey Loewenstein’s rule, *i.e.* two substitution sites cannot be adjacent. The simulation cell consists of two clay platelets of 32 unit-cells each: four in the  $x$  dimension and eight in the  $y$  dimension and hence the system contains two interlayer spaces. The basal surface is  $\sim 42.24 \text{ \AA} \times 36.56 \text{ \AA}$  (Figure 1a) and the clay sheet is  $6.56 \text{ \AA}$  thick. Initially, the basal spacing is set at  $18 \text{ \AA}$ , which is large enough to adapt the ions with long chains.

Figure 1b shows the alkylammonium models by taking the C<sub>8</sub>, C<sub>13</sub> and C<sub>18</sub> ions as examples. Figure 1b shows the optimized configurations, with the geometry optimization performed using the LAMMPS package (Plimpton, 1995) with CVFF by taking 1.0E-4 as the energy-change tolerance. In our simulations, it is assumed that the natural interlayer ions (usually Na<sup>+</sup>) were fully replaced by alkylammonium ions. As the initial configurations, the alkylammonium ions were placed randomly in the interlayer regions. For those cases involving water, the water content was set at  $\sim 1\%$  (16 water molecules in each interlayer space) based on previous TGA measurements of organoclays (Boulet *et al.*, 2003; Greenwell *et al.*, 2005), and water molecules were inserted randomly with the ions.

### Simulation details

The total energy of the hybrid system can be expressed as (Perry *et al.*, 2006; Cygan, 2001)

$$E_{\text{total}} = E_{\text{Coul}} + E_{\text{VDW}} + E_{\text{bond stretch}} + E_{\text{bond bend}} + E_{\text{torsion}} \quad (1)$$

where  $E_{\text{Coul}}$  and  $E_{\text{VDW}}$  stand for the non-bonded coulombic interaction and the Van der Waals term, respectively;  $E_{\text{bond stretch}}$ ,  $E_{\text{bond bend}}$  and  $E_{\text{torsion}}$  denote the bonded terms: bond stretching, bond bending and torsion, respectively. The first three terms are used to calculate the energy of smectite based on clayff. All terms are evaluated for representing the organic ions based on CVFF. Water is represented by the SPC model (Berendsen *et al.*, 1981; Teleman *et al.*, 1987), which is consistent with both clayff and CVFF. In the simulation, a  $12.0 \text{ \AA}$  cut-off is used for the short-range interactions. The electrostatic interaction is treated using the Ewald summation (Frenkel and Smit, 2002) and the number of K-space vectors is determined to reach a precision of 1.0E-4 in conjunction with the pair-wise calculation within a cut-off of  $12.0 \text{ \AA}$ .

All mean displacement simulations were carried out using the LAMMPS package (Plimpton, 1995). To obtain the swelling curve, we performed NPT (298 K, 1 atm) simulations for systems intercalated by alkylammoniums of the alkyl chain length ranging from 6 to 18. Each simulation was performed first for 1500 ps, and then a production stage of 500 ps simulation was performed in order to record the results. Those systems containing water were also relaxed with this procedure. Then, to derive the structural and dynamic properties, a further

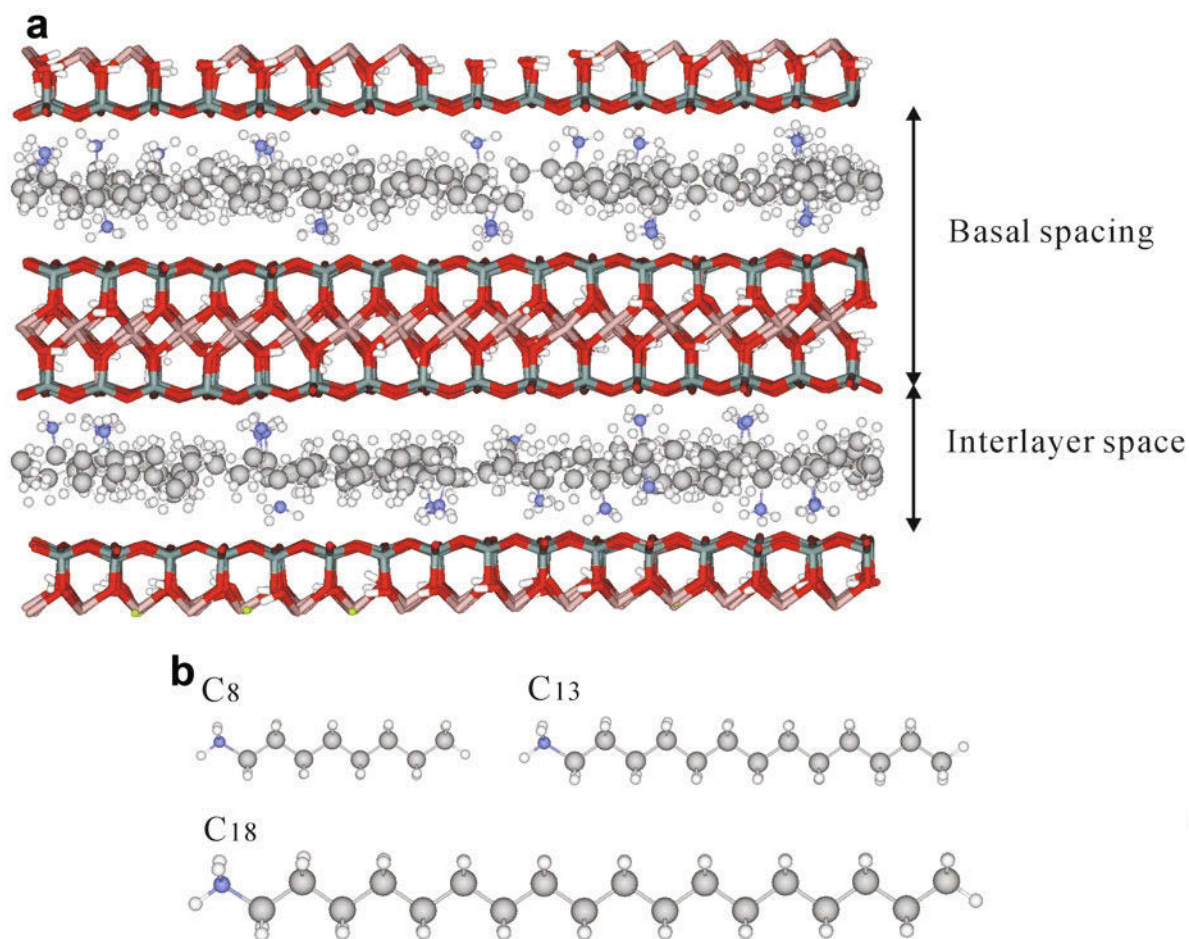


Figure 1. (a) Snapshot of smectite intercalated by  $C_8$ -alkylammoniums; (b) optimized geometries of alkylammonium ions with alkyl chain lengths of 8, 13 and 18. The stick frame represents the clay structure; for the alkylammoniums, H = white, N = gray and C = light gray.

500 ps NVT (298 K) simulation was performed following the previous 2000 ps NPT simulation. A time step of 1.0 fs was used for all simulations and an interval of 100 fs was used to record trajectories. In each simulation run, all atoms were allowed to move.

#### Data analysis

The basal spacing value ( $b$ ) is calculated from the production NPT steps

$$b = \langle V \rangle / (2 \times S) \quad (2)$$

where  $\langle V \rangle$  denotes the statistically averaged volume and  $S$  is the basal surface area.

The spatial distributions of interlayer species are characterized by the atomic density profiles along the  $z$  direction (perpendicular to the basal plane of clay), calculated by averaging over the NVT trajectories. Taking the plane defined by the average bottom octahedral oxygen positions in Figure 1 as the origin ( $z = 0$ ), the density distribution reads

$$\rho(z) = \langle N(z - \Delta z/2, z + \Delta z/2) \rangle / (\Delta z \times S) \quad (3)$$

Here  $\langle N(z - \Delta z/2, z + \Delta z/2) \rangle$  the averaged atom number occurring in the height interval  $(z - \Delta z/2, z + \Delta z/2)$  ( $\Delta z = 0.2 \text{ \AA}$  in this study).

The density of the organic phase formed by the alkyl chains is calculated as follows

$$D = m / (S \times (b - h \times 2)) \quad (4)$$

where  $m$  denotes the mass of the alkyl chains,  $S$  is the area of the basal surface,  $b$  is the basal spacing and  $h$  is the average distance of the organic phase from the clay surface.  $h$  is taken as 4.8  $\text{\AA}$ , based on the density profiles (Figure 3) where it can be observed that the alkyl chains in all systems are all limited in the spaces  $\sim 4.8 \text{ \AA}$  from the ( $z = 0$ ) plane.

The radial distribution function (RDF) for species  $B$  around  $A$  is calculated as (Allen and Tildesley, 1987)

$$G_{AB}(r) = \frac{1}{4\pi\rho_B r^2} \frac{dn_{AB}}{dr} \quad (5)$$

where  $\rho_B$  is the number density of species  $B$ , and  $dn_{AB}$  is the average number of particles of type  $B$  lying at the distances of  $r$  to  $r+dr$  from a particle of  $A$ .

The self-diffusion coefficients,  $D$ , of the interlayer species can be calculated with the Einstein relation (Allen and Tildesley, 1987; Chang *et al.*, 1997)

$$\frac{1}{N} \sum_{i=1}^N \langle |\mathbf{r}_i(t) - \mathbf{r}_i(0)|^2 \rangle = 2dDt \quad (6)$$

where  $N$  is the atom number and  $\mathbf{r}_i(t)$  is the center-of-mass position of the  $i$ th one at time  $t$ ;  $d$  is the diffusion dimension, *i.e.*  $d = 3$  for the total coefficient and  $d = 1$  for the component coefficient on the separate  $x$ ,  $y$  or  $z$  direction. The left-hand side of equation 6 is usually termed as the mean squared displacement (MSD). The separate MSD contribution on each direction is derived and denoted as  $XX$ ,  $YY$  and  $ZZ$ . The contribution of the movement parallel to the  $x$ - $y$  plane is calculated as  $(XX+YY)/2$  and denoted simply as  $XY$ .

## RESULTS

### Swelling curves

Figure 2 shows the simulated and experimental swelling curves. The experimental data are from XRD analysis of the intercalated smectites of the similar layer-charge characteristic to our model (Laird *et al.*, 1989). The swelling curve represents the typical step-wise behavior and shows monolayers up to carbon chain length of 12, intermediate states for chain lengths of 13 to 15 and bilayers for the longer chains. The simulated results are in good accord with the experimental data

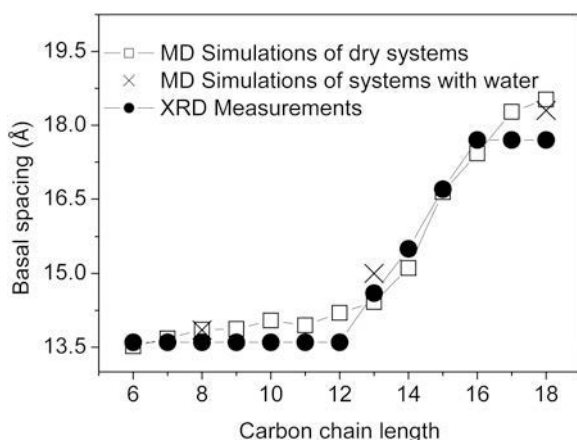


Figure 2. Swelling curves of alkylammonium-smectites. Experimental data are from Laird *et al.* (1989). The error bars are smaller than the symbol size. The lines between the data are to guide the eye.

throughout the tested chain lengths and the discrepancy at each chain length is  $<5\%$ . Furthermore, the basal spacing values of the systems with water are very close to those of corresponding dry systems, indicating that the current water amount cannot alter the interlayer spacing.

### Density distributions and densities of organic phases

All intercalated atomic species present clear peaks on the density distribution profiles (Figure 3). For the systems without water, the locations of the peaks of ammonium N are  $\sim 1.4$  Å from the clay surfaces (the section of  $\sim 0$ – $3.28$  Å on the  $z$  axis is for the clay phase). The hydrocarbon chains are further away from the surfaces and they typically represent layering behavior. In the  $C_8$  system, the two single peaks of carbon chains denote the monolayer configurations (snapshot in Figure 1), whereas in the  $C_{13}$  system, slight splits occur in the two single peaks. But for the case of  $C_{18}$ , double peaks are well defined in each interlayer space, indicating the formation of double layers.

In the systems containing water, the distributions of ammonium groups vary clearly: some small peaks occur relatively far away from the surfaces besides those considerable groups that are still adjacent to the surfaces. In contrast, the peaks of the hydrocarbon chains retain their shapes as in the dry systems, implying that water does not impose significant influence on the layering behaviors of the chains. Water molecules represent two peaks in each interlayer gallery and their locations are  $\sim 2.2$  Å from the surfaces, between those of ammoniums and hydrocarbon chains.

The densities of the interlayer organic phases in the systems of  $C_{11-14}$ , are greater than those of the other systems (Figure 4). This indicates that in the  $C_{11-14}$  systems, the alkyl chains are densely packed and the organic phases formed are very compact, whereas in the other systems the organic phases are relatively loose. This is also consistent with the density profiles of the alkyl chains, where the peak values in the  $C_{13}$  systems are much greater than those of the  $C_8$  and  $C_{18}$  systems (Figure 3).

### Radial distribution functions (RDFs)

Figure 5 illustrates the derived RDFs for surface O (SO) around ammonium H (AH) in both dry and 'wet' systems ( $G_{AH-SO}(r)$  in Figure 5a,b,c), water O (WO) around ammonium H ( $G_{AH-WO}(r)$  in Figure 5d) and surface O around water H (WH) ( $G_{WH-SO}(r)$  in Figure 5e) in the three systems with water. The three profiles of  $G_{AH-SO}(r)$  in the dry systems present similar and sharp peaks and the two to the left are located at  $\sim 2$  Å and  $3.9$  Å, respectively. The  $G_{AH-SO}(r)$  RDFs in the systems with water retain the profiles in the corresponding dry systems but the two peaks to the left clearly decrease relative to those in the dry systems. In the systems with water, the three  $G_{AH-WO}(r)$  RDFs in

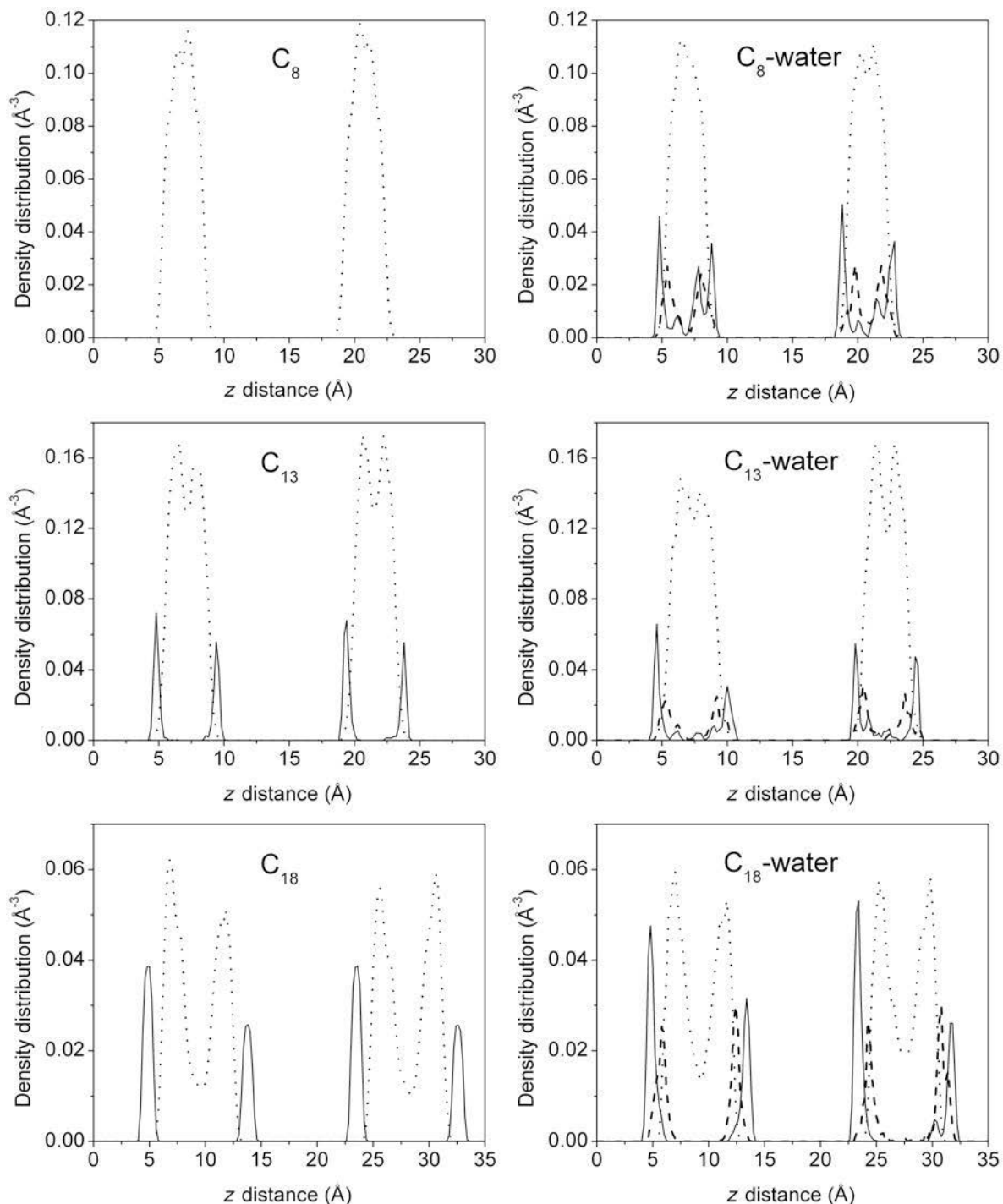


Figure 3. Density distribution profiles of interlayer atomic species in the organoclays of the three selected carbon chain lengths. Dotted line: C of alkyl chains; solid line: ammonium N; dashed line: water O. The intensity of the density profiles of ammonium N and water O are increased by a factor of five for the purpose of clarity.

Figure 5d present two clear peaks: one centered at 1.97 Å and the other at ~3.5 Å. There are no peaks well defined on  $G_{\text{WH-SO}}(r)$  RDFs (Figure 5e), suggesting that there is no strong bonding between water and the clay surface.

#### Mean square displacements (MSDs)

In the six simulated systems, the MSDs of the alkyl species always reach plateaux after ~200–300 ps and obviously the ammoniums have much smaller MSDs than the alkyl chains (Figure 6). In the three systems

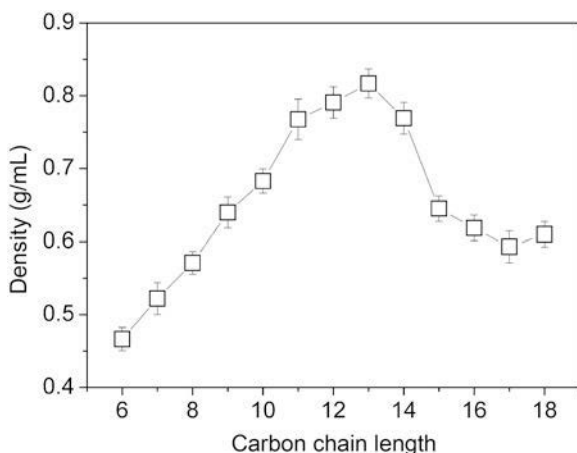


Figure 4. Densities of the organic phases in the organoclays. The lines between the data points are to guide the eye.

with water, water presents larger MSDs than alkyls and ammoniums. Notably, the cases of the  $C_{13}$  systems are very special: the MSD plateaux of the alkyl species are only  $\sim 2.5 \text{ \AA}^2$ , much less than those of the  $C_8$  and  $C_{18}$  systems and the MSDs of water are also much less than those of water in the other two systems with water.

The separate contributions of the MSDs of the  $C_{18}$  systems are shown in Figure 7 and the other systems have qualitatively similar trends. In the dry system, the ZZ and XY components of the ammonium groups are both  $< 0.1 \text{ \AA}^2$ . In the system with water, the XY component of the ammoniums is a little greater than that of the ZZ, but the magnitude is still  $< 1 \text{ \AA}^2$ . For alkyl chain groups, the XY components are larger than the ZZ ones in both the dry and wet systems. The same trend is observed for water molecules. These findings reflect confinement effects of the interlayer space: The potential barriers caused by the two opposite smectite surfaces limit the movement in the  $z$  direction, but the direction in the  $xy$  plane is relatively open (Skipper *et al.*, 2006).

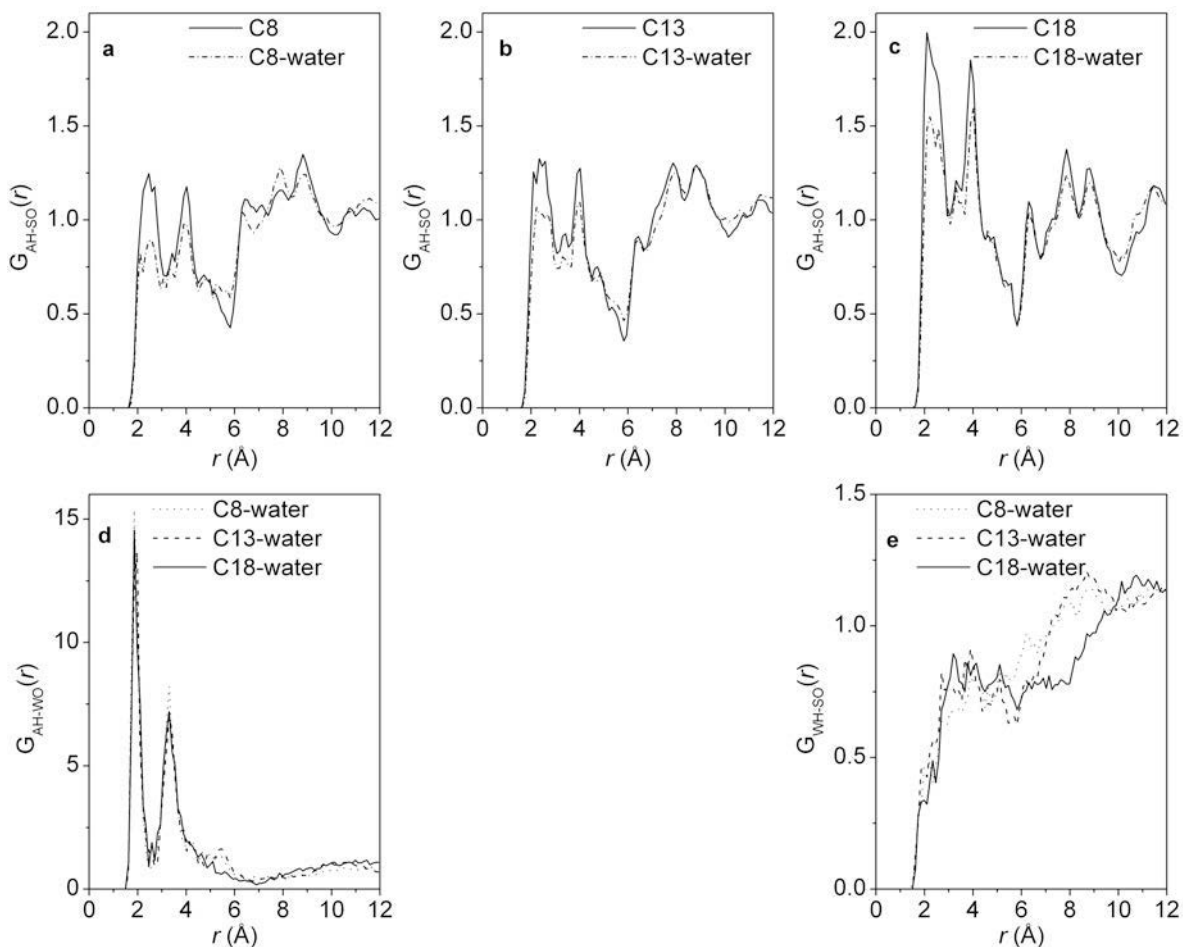


Figure 5. Radial distribution functions: (a, b, c) surface oxygen around ammonium H; (d) water O around ammonium H; (e) surface oxygen around water H. AH – ammonium H; SO – surface oxygen; WO – water oxygen; WH – water H.

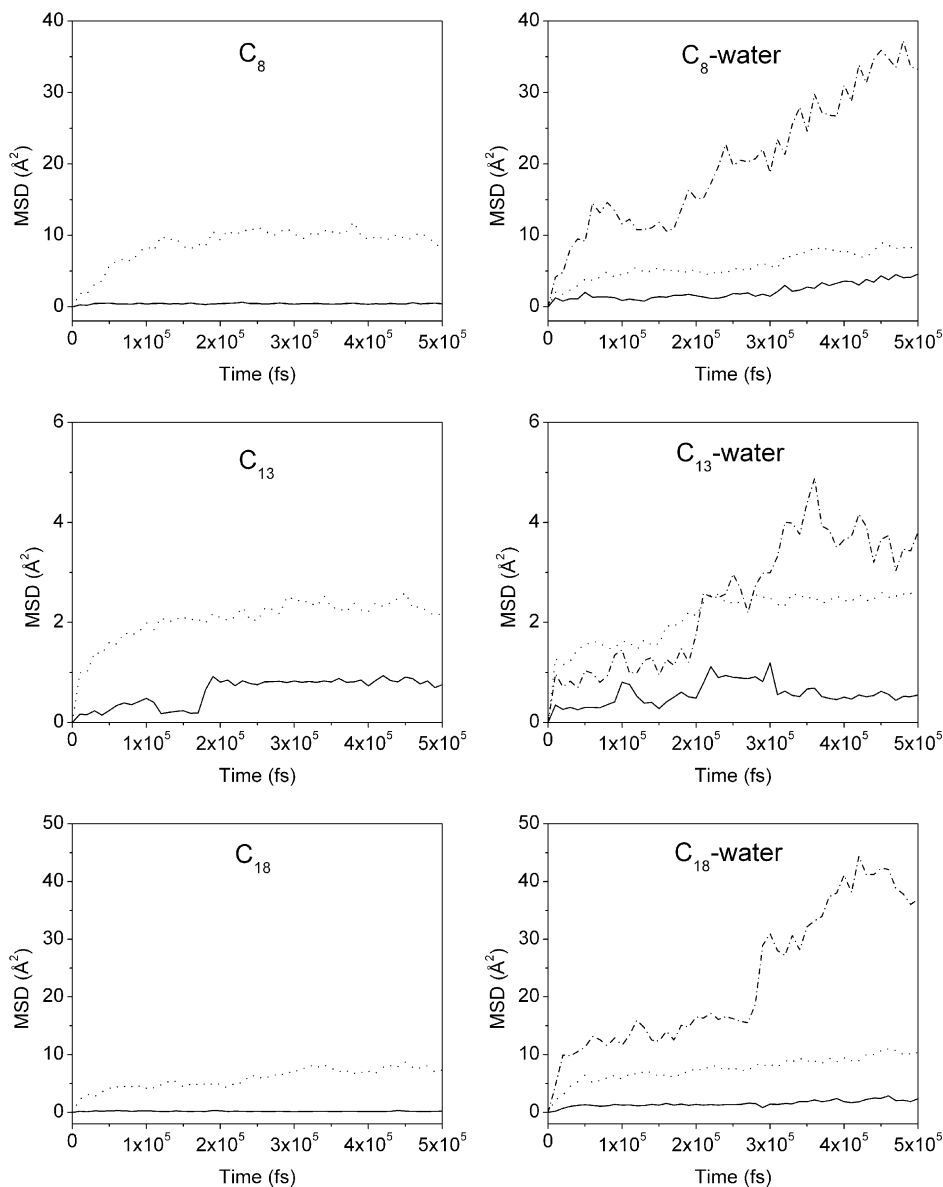


Figure 6. Mean square displacements of interlayer species in the organoclays. Dotted line – alkyl groups; solid line – ammonium groups; dashed line – water O.

## DISCUSSION

### *Validation of the force field*

The simulated basal spacing values agree well with the experimental data and the derived density profiles in Figure 3 disclose the layering behaviors of alkyl chains, corresponding well with the proposed monolayer, transition and bilayer configurations. These results validate the combined clayff-CVFF force field in the simulations of the hybrid systems and thus assure the further analyses of the interlayer structures and dynamics.

The interfaces between minerals and organics are of great interest in many fields (*e.g.* geochemistry and

material sciences) and the force field-based molecular simulations are very powerful techniques to gain insights into these complex systems. The current validation, together with previous studies (Kumar *et al.*, 2006; Cygan *et al.*, 2004b), demonstrates that it is feasible to study these interfaces using the clayff-CVFF. The clayff is superior for exploring microscopic properties at the atomic level for the accurate parameterizations of atomic interactions and furthermore it is suitable for simulating a wide spectrum of minerals, including oxides, oxyhydroxides and the clay family (Cygan *et al.*, 2004b). On the other hand, the atomically detailed CVFF can simulate very complex organic systems including proteins (Dauber-Osguthorpe *et al.*, 1988). Therefore it is

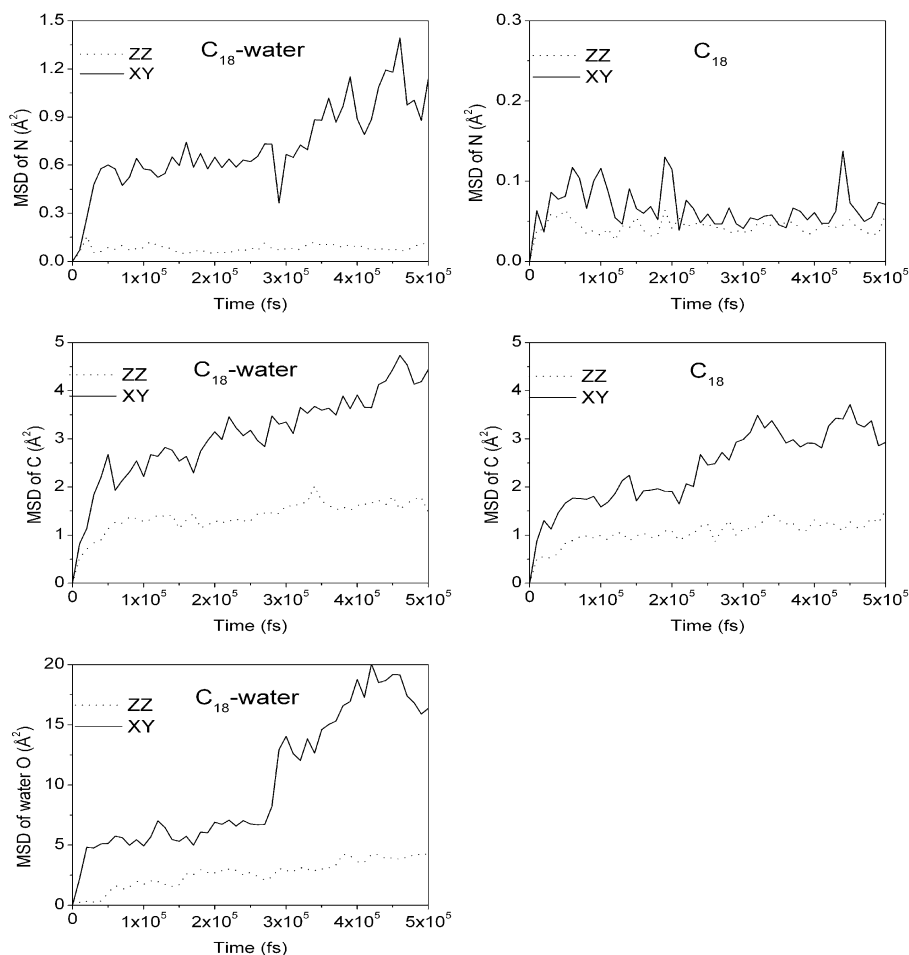


Figure 7. Separate mean square displacement components of interlayer species in the  $C_{18}$  organoclays. ZZ: the MSD component in the direction perpendicular to the basal surface; XY: the MSD component in the direction parallel to the basal surface.

believed that the combined force field is able to facilitate the studies of the mineral-organic interfaces.

#### Interlayer bonding

The clear peaks of  $G_{AH-SO}(r)$  illustrated in Figure 5(a,b,c) indicate that there exist strong interactions between ammonium H and surface O. In fact, detailed analyses of trajectories demonstrate that ammonium groups all locate above the surface six-member rings with the H atoms forming hydrogen bonds with surface O atoms to maximize the attractions. The snapshot in Figure 8a depicts the distribution of ammonium groups and the inset shows the orientations. This observation confirms the experimental report (Lagaly and Weiss, 1970) and is consistent with that found in the simulation of the smectite intercalated by poly (propylene oxide)-ammonium (Greenwell *et al.*, 2005). It is also clear that the first peak of the  $G_{AH-SO}(r)$  denotes the coordination of ammonium H with the three frontal surface O atoms and the second peak denotes H atoms correlating with surface O from neighboring siloxane rings.

In the systems with water, the decreases in the two left peaks of the  $G_{AH-SO}(r)$  (dotted curves in Figure 5a,b,c) indicate that some ammonium groups move away from the surface oxygen. This corresponds with the variations of the ammonium density profiles in Figure 3. Moreover, the snapshot (Figure 8b) shows that the distribution of ammonium groups varies in the plane parallel to the basal surface. The first peaks of  $G_{AH-WO}(r)$  RDFs (Figure 5d) have widths  $<0.7 \text{ \AA}$ . These very sharp peaks indicate that strong hydrogen bonds have formed between ammonium H and water O and the inset of Figure 8b illustrates these H bonds. So, it is clear that the water molecules drag some ammonium groups away from the clay surfaces and reduce the correlation between ammonium H and surface O.

#### Dynamics

The MSD patterns of alkyl chains and the ammoniums typically indicate that their motions are very restricted (Refson *et al.*, 1993). In the dry systems, the extremely small magnitude of the MSD components of the ammoniums ( $\sim 0.1 \text{ \AA}^2$ ) indicates that these groups are



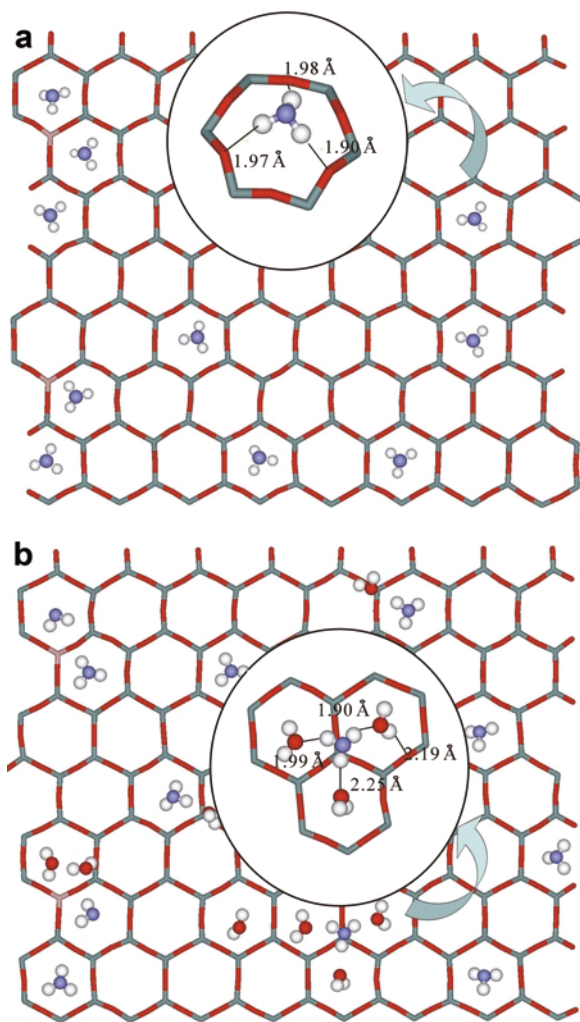


Figure 8. Snapshots from the simulations of smectites intercalated by: (a)  $C_{13}$  ammoniums; and (b)  $C_{18}$  ammoniums and water. Both figures are viewed from the direction perpendicular to the basal surface. The alkyl chains are not shown for clarity.

fixed firmly and cannot overstep the potential barriers produced by the surface six-member rings. In the systems with water, the XY component of ammonium groups is a little greater but the magnitude is still  $<1 \text{ \AA}^2$ , demonstrating that they are still very immobile although some groups can move to the higher locations (Figure 3). In the dry systems, the carbon chains are more mobile than the ammonium groups and the cases are similar in the systems with water. This shows that water does not impact the mobility of alkyl chains significantly. So, under the ambient conditions, the ammonium groups are in fact anchored firmly on the clay surfaces and the carbon chains are just a little more mobile in organic phases. This is very similar to the NMR study of the cadmium thiophosphates intercalated by cetyl trimethyl ammonium ions (Suresh *et al.*, 2003), where it was observed that the polar heads are more immobile than the alkyl tails. The staggered MSD styles

of water show that their motions are also limited, mainly due to the strong interactions with ammonium groups from the discussions above in section 4.2. Fitting the MSD data after  $2 \times 10^5$  fs of the  $C_8$ -water system gives the coefficient  $1.3 \times 10^{-10} \text{ m}^2/\text{s}$ , which is much less than the bulk value  $2.3 \times 10^{-9} \text{ m}^2/\text{s}$  (Ohtaki and Radnai, 1993).

The extreme rigidity in the  $C_{13}$  system is found to be due to the very dense interlayer structures. The atom distribution profiles and the calculated densities show that the alkyl chains are densely packed in the interlayer space. To confirm the correspondence between the density and the mobility, we performed additional simulations with the  $C_{10}$ ,  $C_{12}$  and  $C_{15}$  systems and found that the MSDs of the  $C_{10}$  and  $C_{15}$  chains are very close to those of  $C_8$  and  $C_{18}$  and the MSD of  $C_{12}$  is near to that of  $C_{13}$ . So it can be deduced that there is the similar rigidity in the systems of alkyl chain lengths of 11 to 14, which have the greatest densities (Figure 4). Similar results were found for systems with water. Since the unfilled space in the  $C_{13}$ -water system is much less than the other two systems (the density files in Figure 3), the diffusion of water molecules is very limited and represents relatively lower mobility in Figure 6.

## CONCLUSIONS

The mean displacement simulations were performed to study the interlayer structures and dynamics of alkylammonium-intercalated smectites. The combined clayff-CVFF force field is validated in simulating these hybrid materials. The current validation and several previous studies show that the clayff-CVFF is feasible for use in the simulations of a wide range of the complex mineral-organic interfaces.

In the systems without water, the layering behaviors of alkyl chains are clearly seen. The alkylammonium groups are all anchored firmly above the surface six-member rings through H bonds between ammonium H and surface O, and the alkyl tails are more mobile. In the systems with water, water O tends to form H bonds with ammonium H and these strong interactions drag some ammoniums out of the potential barriers of the six-member rings. Water scarcely affects the basal spacing, the layering behaviors of alkyl chains or the dynamics of alkylammoniums. So, even in the presence of water, the organic ions are still fixed in the interlayer gallery. The mobility of water is much less than in the bulk case, which is mainly due to the coordination with the ammoniums.

The intercalated species are found to be extremely rigid in the systems of the alkyl chain lengths of 11 to 14 and the density analyses highlight the correspondence between the density and the rigidity. In those systems, the alkyl chains are densely packed with high densities, whereas in other systems the organic phases are relatively loose and there is more space available.

## ACKNOWLEDGMENTS

The authors acknowledge the anonymous reviewers for their constructive comments. This study was supported by the National Science Foundation of China (No. 40373024 and 40673041) and the Scientific Research Foundation of the Graduate School of Nanjing University.

## REFERENCES

- Allen, M.P. and Tildesley, D. J. (1987) *Computer Simulation of Liquids*. Clarendon Press: Oxford, UK.
- Berendsen, H.J.C., Postma, J.P.M., van Gunsteren, W.F. and Hermans, J. (1981) Interaction models for water in relation to protein hydration. Pp. 331–342 in: *Intermolecular Forces* (B. Pullman, editor). Riedel, Dordrecht, The Netherlands.
- Boulet, P., Bowden, A.A., Coveney, P.V. and Whiting, A. (2003) Combined experimental and theoretical investigations of clay polymer nanocomposites: intercalation of single bifunctional organic compounds in Na<sup>+</sup>-montmorillonite and Na<sup>+</sup>-hectorite clays for the design of new materials. *Journal of Materials Chemistry*, **13**, 2540–2550.
- Carrizosa, M.J., Rice, P.J., Koskinen, W.C., Carrizosa, I. and Hermosin, M.D. (2004) Sorption of isoxaflutole and DKN on organoclays. *Clays and Clay Minerals*, **52**, 341–349.
- Chang, F.-R.C., Skipper, N.T. and Sposito, G. (1997) Monte Carlo and molecular dynamics simulations of interfacial structure in lithium-montmorillonite hydrates. *Langmuir*, **13**, 2074–2082.
- Cygan, R.T. (2001) Molecular modeling in mineralogy and geochemistry. Pp. 1–35 in: *Molecular Modeling Theory: Applications in the Geosciences* (R.T. Cygan and J.D. Kubicki, editors). Reviews in Mineralogy and Geochemistry, **42**, Mineralogical Society of America.
- Cygan, R.T., Guggenheim, S. and van Groos, A.F.K. (2004a) Molecular models for the intercalation of methane hydrate complexes in montmorillonite clay. *Journal of Physical Chemistry B*, **108**, 15141–15149.
- Cygan, R.T., Liang, J.-J. and Kalinichev, A.G. (2004b) Molecular models of hydroxide, oxyhydroxide, and clay phases and the development of a general force field. *Journal of Physical Chemistry B*, **108**, 1255–1266.
- Dauber-Osguthorpe, P., Roberts, V.A., Osguthorpe, D.J., Wolff, J., Genest, M. and Hagler, A.T. (1988) Structure and energetics of ligand binding to proteins: E. coli dihydrofolate reductase-trimethoprim, a drug-receptor system. *Proteins: Structure, Function and Genetics*, **4**, 31–47.
- Frenkel, D. and Smit, B. (2002) *Understanding Molecular Simulation*, 2nd edition. Academic Press, New York.
- Greathouse, J.A., Stellallevinsohn, H.R., Denecke, M.A., Bauer, A. and Pabalan, R.T. (2005) Uranyl surface complexes in a mixed-charge montmorillonite: Monte Carlo computer simulation and polarized XAFS results. *Clays and Clay Minerals*, **53**, 278–286.
- Greenwell, H.C., Harvey, M.J., Boulet, P., Bowden, A.A., Coveney, P.V. and Whiting, A. (2005) Interlayer structure and bonding in nonswelling primary amine intercalated clays. *Macromolecules*, **38**, 6189–6200.
- Hackett, E., Manias, E. and Giannelis, E.P. (1998) Molecular dynamics simulations of organically modified layered silicates. *Journal of Chemical Physics*, **108**, 7410–7415.
- He, H.P., Galy, J. and Gerard, J. F. (2005) Molecular simulation of the interlayer structure and the mobility of alkyl chains in HDTMA(+)/montmorillonite hybrids. *Journal of Physical Chemistry B*, **109**, 13301–13306.
- Heinz, H., Castelijns, H.J. and Suter, U.W. (2003) Structure and phase transitions of alkyl chains on mica. *Journal of the American Chemical Society*, **125**, 9500–9510.
- Heinz, H., Koerner, H., Anderson, K.L., Vaia, R.A. and Farmer, B.L. (2005) Force field for mica-type silicates and dynamics of octadecylammonium chains grafted to montmorillonite. *Chemistry of Materials*, **17**, 5658–5669.
- Heinz, H., Vaia, R.A., Krishnamoorti, R. and Farmer, B.L. (2007) Self-assembly of alkylammonium chains on montmorillonite: Effect of chain length, head group structure, and cation exchange capacity. *Chemistry of Materials*, **19**, 59–68.
- Horn, R.G. and Israelachvili, J.N. (1981) Direct measurement of forces due to structure in a non-polar liquid. *Journal of Chemical Physics*, **75**, 1400–1411.
- Janek, M. and Smrcok, L. (1999) Application of an internal standard technique by transmission X-ray diffraction to assess layer charge of a montmorillonite by using the alkylammonium method. *Clays and Clay Minerals*, **47**, 113–118.
- Jorgensen, W.L. and Gao, J.L. (1986) Monte Carlo simulations of the hydration of ammonium and carboxylate ions. *Journal of Physical Chemistry*, **90**, 2174–2182.
- Jorgensen, W.L., Madura, J.D. and Swenson, C.J. (1984) Optimized intermolecular potential functions for liquid hydrocarbons. *Journal of the American Chemical Society*, **106**, 6638–6646.
- Kirkpatrick, R.J., Kalinichev, A.G., Hou, X. and Struble, L. (2005) Experimental and molecular dynamics modeling studies of interlayer swelling: water incorporation in kanemite and ASR gel. *Materials and Structures*, **38**, 449–458.
- Kumar, P.P., Kalinichev, A.G. and Kirkpatrick, R.J. (2006) Hydration, swelling, interlayer structure, and hydrogen bonding in organolayered double hydroxides: Insights from molecular dynamics simulation of citrate-intercalated hydrotalcite. *Journal of Physical Chemistry B*, **110**, 3841–3844.
- Lagaly, G. (1981) Characterization of clays by organic compounds. *Clay Minerals*, **16**, 1–21.
- Lagaly, G. (1994) Layer charge determination by alkylammonium ions. Pp. 1–46 in: *Layer Charge Characteristics of Clays* (A. Mermut, editor). CMS Workshop Lectures, **6**, The Clay Minerals Society, Boulder, Colorado.
- Lagaly, G. and Weiss, A. (1970) Anordnung und Orientierung kationischer Tenside auf ebenen Silicatoberflächen. II. Paraffinähnliche Strukturen bei den n-Alkylammonium-Schichtsilicaten mit hoher Schichtladung (Glimmer). *Kolloid Z. Z. Polymere*, **237**, 364–368.
- Lagaly, G., Ogawa, M. and Dekany, I. (2006) Clay mineral organic interactions. Pp. 309–377 in: *Handbook of Clay Science* (F. Bergaya, B.K.G. Theng, and G. Lagaly, editors). Elsevier, Amsterdam.
- Laird, D.A. (1994) Evaluation of the structural formula and alkylammonium methods of determining layer charge. Pp. 80–103 in: *Layer Charge Characteristics of Clays* (A.R. Mermut, editor). CMS Workshop Lectures, **6**, The Clay Minerals Society, Boulder, Colorado.
- Laird, D.A., Scott, A.D. and Fenton, T.E. (1989) Evaluation of the alkylammonium method of determining layer charge. *Clays and Clay Minerals*, **37**, 41–46.
- Liu, X.D. and Lu, X.C. (2006) A thermodynamic understanding of clay-swelling inhibition by potassium ions. *Angewandte Chemie International Edition*, **45**, 6300–6303.
- Mayo, S.L., Olafson, B.D. and Goddard, W.A., III. (1990) DREIDING: a generic force field for molecular simulations. *Journal of Physical Chemistry*, **94**, 8897–8909.
- Mermut, A.R. and Lagaly, G. (2001) Baseline studies of The Clay Minerals Society Source Clays: layer-charge determination and characteristics of those minerals containing 2:1 layers. *Clays and Clay Minerals*, **49**, 393–397.
- Ohtaki, H. and Radnai, T. (1993) Structure and dynamics of hydrated ions. *Chemical Reviews*, **93**, 1157–1204.
- Osman, M.A., Seyfang, G. and Suter, U.W. (2000) Two-

- dimensional melting of alkane monolayers ionically bonded to mica. *Journal of Physical Chemistry B*, **104**, 4433–4439.
- Osman, M.A., Ernst, M., Meier, B.H. and Suter, U.W. (2002) Structure and molecular dynamics of alkane monolayers self-assembled on mica platelets. *Journal of Physical Chemistry B*, **106**, 653–662.
- Osman, M.A., Plöetzle, M. and Skrabal, P. (2004) Structure and properties of alkylammonium monolayers self-assembled on montmorillonite platelets. *Journal of Physical Chemistry B*, **108**, 2580–2588.
- Perry, T.D., Cygan, R.T. and Mitchell, R. (2006) Molecular models of alginic acid: Interactions with calcium ions and calcite surfaces. *Geochimica et Cosmochimica Acta*, **70**, 3508–3532.
- Plimpton, S.J. (1995) Fast parallel algorithms for short-range molecular dynamics. *Journal of Computational Physics*, **117**, 1–19 ([www.cs.sandia.gov/~sjplimp/lammps.html](http://www.cs.sandia.gov/~sjplimp/lammps.html)).
- Refson, K., Skipper, N.T. and McConnell, J.D.C. (1993) Molecular dynamics simulation of water mobility in smectites. Pp. 63–77 in: *Geochemistry of Clay-Pore Fluid Interactions* (D.A.C. Manning, P.L. Hall and C.R. Hughes, editors). Mineralogical Society Series, **4**. Chapman & Hall, London.
- Skipper, N.T., Chang, F.-R. and Sposito, G. (1995) Monte Carlo simulation of interlayer molecular structure in swelling clay minerals. 1. Methodology. *Clays and Clay Minerals*, **43**, 294–303.
- Skipper, N.T., Lock, P.A., Titiloye, J.O., Swenson, J., Mirza, Z.A., Howells, W.S. and Fernandez-Alonso, F. (2006) The structure and dynamics of 2-dimensional fluids in swelling clays. *Chemical Geology*, **230**, 182–196.
- Suresh, R., Vasudevan, S. and Ramanathan, K.V. (2003) Dynamics of methylene chains in an intercalated surfactant bilayer by solid-state NMR spectroscopy. *Chemical Physics Letters*, **371**, 118–124.
- Tambach, T.J., Hensen, E.J.M. and Smit, B.J. (2004) Molecular simulations of swelling clay minerals. *Journal of Physical Chemistry B*, **108**, 7586–7596.
- Tambach, T.J., Boek, E.S. and Smit, B. (2006) Molecular order and disorder of surfactants in clay nanocomposites. *Physical Chemistry Chemical Physics*, **8**, 2700–2702.
- Teleman, O., Jonsson, B. and Engstrom, S. (1987) A molecular dynamic simulation of a water model with intramolecular degrees of freedom. *Molecular Physics*, **60**, 193–203.
- Vaia, R.A., Teukolsky, R.K. and Giannelis, E.P. (1994) Interlayer structure and molecular environment of alkylammonium layered silicates. *Chemistry of Materials*, **6**, 1017–1022.
- Wang, J.W., Kalinichev, A.G. and Kirkpatrick, R.J. (2004) Molecular modeling of water structure in nano-pores between brucite (001) surfaces. *Geochimica et Cosmochimica Acta*, **68**, 3351–3365.
- Wang, J.W., Kalinichev, A.G. and Kirkpatrick, R.J. (2006) Effects of substrate structure and composition on the structure, dynamics, and energetics of water at mineral surfaces: A molecular dynamics modeling study. *Geochimica et Cosmochimica Acta*, **70**, 562–582.
- Wang, L.Q., Liu, J., Exarhos, G.J., Flanagan, K.Y. and Bordia, R. (2000) Conformation heterogeneity and mobility of surfactant molecules in intercalated clay minerals studied by solid-state NMR. *Journal of Physical Chemistry B*, **104**, 2810–2816.
- Weiss, A. (1963) Organic derivatives of mica-type layer silicates. *Angewandte Chemie International Edition*, **2**, 134–144.
- Zeng, Q.H., Yu, A.B., Lu, G.Q. (Max) and Standish, R.K. (2003) Molecular dynamics simulation of organic-inorganic nanocomposites: the layering behavior and interlayer structure of organoclays. *Chemistry of Materials*, **15**, 4732–4738.
- Zeng, Q.H., Yu, A.B., Lu, G.Q. (Max) and Standish, R.K. (2004) Molecular dynamics simulation of the structural and dynamic properties of organoclay. *Journal of Physical Chemistry B*, **108**, 10025–10033.
- Zhu, J.X., He, H.P., Zhu, L.Z., Wen, X.Y. and Deng, F. (2005) Characterization of organic phases in the interlayer of montmorillonite using FTIR and C-13 NMR. *Journal of Colloid and Interface Science*, **286**, 239–244.

(Received 23 May 2007; revised 28 August 2007; Ms. 0034; A.E. Will P. Gates)